

Single-step quantum state engineering in traveling optical fields

Gabor Mogyorosi,¹ Peter Adam,^{1,2} Emese Molnar,¹ and Matyas Mechler¹

¹*Institute of Physics, University of Pécs, Ifjúság útja 6, H-7624 Pécs, Hungary*

²*Institute for Solid State Physics and Optics, Wigner Research Centre for Physics, Hungarian Academy of Sciences, P.O. Box 49, H-1525 Budapest, Hungary*



(Received 25 April 2018; revised manuscript received 10 April 2019; published 25 July 2019)

We propose an experimental quantum state engineering scheme for the high-fidelity conditional generation of various nonclassical states of practical relevance in traveling optical fields. It contains a single measurement, thereby achieving a high success probability. The generated state is encoded in the optimal choice of the physically controllable parameters of the arrangement. These parameter values are determined via numerical optimization.

DOI: [10.1103/PhysRevA.100.013851](https://doi.org/10.1103/PhysRevA.100.013851)

I. INTRODUCTION

Nonclassical states of light play an essential role in numerous applications in optical quantum information processing, quantum-enhanced metrology, and fundamental tests of quantum mechanics. Measurement-induced conditional preparation is an efficient method for generating quantum states of traveling optical fields required in many of these applications. This consists in the measurement of one of the modes of a bipartite correlated state, thereby projecting the state of the other mode to the desired one. Most of such conditional schemes have been developed specially for generating optical cat states. Indeed, these states and also their squeezed versions have already been prepared in several traveling-wave experiments [1–6].

The generation of a broader class of relevant nonclassical states requires a more general approach to quantum state engineering, especially for states lacking a specialized preparation scheme. The aim of these general protocols is the preparation of a large variety of states in the same experimental setup [7–14].

It is a common approach, for instance, to construct systematically the photon number expansion of the quantum states up to a given photon number. The methods developed for this task are based on repeated photon additions [8], photon subtractions [9], and various combinations of these [12,15]. In such schemes, the number of the optical elements and detection events is generally proportional to the amount of number states involved in the photon number expansion of the target state. This property obviously leads to a decrease in the success probability and even to that in the fidelity of the preparation of states involving larger photon number components. There have been two quantum state engineering schemes proposed that can overcome this issue [16]. These contain only a few beam splitters and two or three homodyne measurements, and they are capable of preparing nonclassical states by the application of discrete coherent-state superpositions approximating the target states. These schemes, however, still exhibit a moderate success probability due to the application of multiple measurements.

In this paper, we show that a single-step conditional generation scheme using separately prepared squeezed coherent states as inputs can be applied for preparing several types of nonclassical states with high fidelity and success probability. The paper is organized as follows. In Sec. II we describe our proposed scheme, and we determine the general form of the output states. In Sec. III we demonstrate through examples that the proposed scheme is capable of generating various nonclassical states with high performance. Finally, in Sec. IV the results are summarized and conclusions are drawn.

II. THE SINGLE-STEP SCHEME

The proposed conditional scheme is presented in Fig. 1. Two squeezed coherent states $|\zeta_j, \alpha_j\rangle = \hat{D}(\alpha_j)\hat{S}(\zeta_j)|0\rangle$ with squeezing factors $\zeta_j = r_j \exp(i\theta_j)$ and coherent amplitudes $\alpha_j = |\alpha_j| \exp(i\phi_j)$ ($j = 1, 2$) overlap with a $\pi/2$ phase shift on a tunable beam splitter of transmittance T . Then a multi-photon detection (MPD) or a homodyne measurement (HM) measuring the rotated quadrature operator X_λ is performed on one of the outputs to herald the generation of the desired output state $|\psi_{\text{out}}\rangle$ on the other mode. The MPD can be realized by photon number resolving detectors (PNRDs), which are already available devices under intensive development. Transition edge sensors [17,18] and superconducting nanowires [19] may be the most widely known types of PNRDs. These detectors have been used in several successful experiments [4,6,14,20,21]. The projection onto a single-photon state can also be performed with the help of an ancillary single-photon state, a pair of beam splitters, and a pair of homodyne detectors [22].

In the case of MPD the output state is non-Gaussian, while for the scheme with HM it is Gaussian. The significance of the latter scheme is that it can vary the characteristics of the outgoing Gaussian state even at fixed inputs, enabling the generation of various states in a single setup.

The photon number expansions of the output states corresponding to the two types of measurements can be described by the expressions presented in Eqs. (1) and (2) for the

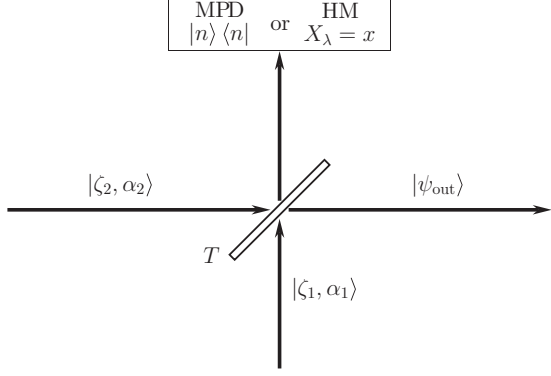


FIG. 1. Experimental scheme with two types of measurements for generating nonclassical states in a traveling optical field. The input states $|\zeta_i, \alpha_i\rangle$ interfering on a beam splitter with transmittance T are squeezed coherent states.

setups containing MPD and HM, respectively, where we have introduced the function $B_p^q(x) = {q \choose p}(\sqrt{x})^{q-p}(\sqrt{1-x})^p$ and the notation $\beta_j = \alpha_j \cosh(r_j) + \alpha_j^* e^{i\theta_j} \sinh(r_j)$. The photon number expansion presented in Eq. (1) contains nine adjustable parameters. These are the complex squeezing parameters ζ_j and the complex coherent signals α_j of the input squeezed coherent states, and the transmittance T of the beam splitter. The other expansion given by Eq. (2) contains another two parameters, namely the measurement results x of the quadrature operator X_λ and the rotation angle λ characterizing this operator. Quantum state engineering of various target states can be realized by the proper choice of these parameters. The optimal choice can be determined by minimizing the misfit $\varepsilon = 1 - |\langle \psi_{out} | \psi_{target} \rangle|^2$ between the desired state $|\psi_{target}\rangle$ and the approximated one $|\psi_{out}\rangle$ that is generated,

$$|\psi_{out}\rangle_{MPD} = \mathcal{N}_{out} \prod_{j=1}^2 \frac{\exp\left(-\frac{1}{2}|\alpha_j|^2 - \frac{1}{2}\alpha_j^{*2}e^{i\theta_j} \tanh(r_j)\right)}{\sqrt{\cosh(r_j)}} \sum_{k=0}^{\infty} \sum_{l=0}^{\infty} \sum_{m=0}^k i^{2m-k+n} \frac{\left(\frac{1}{2}e^{i\theta_1} \tanh(r_1)\right)^{\frac{k}{2}}}{k!} \frac{\left(\frac{1}{2}e^{i\theta_2} \tanh(r_2)\right)^{\frac{l}{2}}}{l!} \\ \times H_k\left(\beta_1[e^{i\theta_1} \sinh(2r_1)]^{-\frac{1}{2}}\right) H_l\left(\beta_2[e^{i\theta_2} \sinh(2r_2)]^{-\frac{1}{2}}\right) B_m^k(T) B_{m+l-n}^l(1-T)\sqrt{n!(k+l-n)!} |k+l-n\rangle, \quad (1)$$

$$|\psi_{out}\rangle_{HM} = \mathcal{N}_{out} \pi^{-\frac{1}{4}} e^{-\frac{1}{2}x^2} \prod_{j=1}^2 \frac{\exp\left(-\frac{1}{2}|\alpha_j|^2 - \frac{1}{2}\alpha_j^{*2}e^{i\theta_j} \tanh(r_j)\right)}{\sqrt{\cosh(r_j)}} \sum_{k=0}^{\infty} \sum_{l=0}^{\infty} \sum_{m=0}^k \sum_{p=0}^l (-1)^p \left(\frac{1}{4}e^{i(\theta_1-2\lambda)} \tanh(r_1)\right)^{\frac{k}{2}} \\ \times \left(-\frac{1}{4}e^{i(\theta_2-2\lambda)} \tanh(r_2)\right)^{\frac{l}{2}} \frac{\sqrt{(m+p)!}}{k!l!} (\sqrt{2}ie^{i\lambda})^{m+p} B_m^k(T) B_p^l(1-T) H_{k+l-(m+p)}(x) H_k\left(\beta_1[e^{i\theta_1} \sinh(2r_1)]^{-\frac{1}{2}}\right) \\ \times H_l\left(\beta_2[e^{i\theta_2} \sinh(2r_2)]^{-\frac{1}{2}}\right) |m+p\rangle. \quad (2)$$

In addition to misfit, the probability of success is another figure of merit characterizing the performance of a conditional scheme. In the case of MPD it is defined as $P = \text{Tr}(\hat{\rho}_3|n\rangle\langle n|)$, while for HM resulting in the measured value x^{opt} , it is defined as

$$P(x^{\text{opt}}, \delta) = \int_{x^{\text{opt}}-\delta}^{x^{\text{opt}}+\delta} \text{Tr}(\hat{\rho}_3|x\rangle\langle x|) dx, \quad (3)$$

where $\hat{\rho}_3 = \text{Tr}_4(|\psi_{out}\rangle_{3434}\langle\psi_{out}|)$ is the density operator of the mode on which the measurement is performed. The two-mode output state after the beam splitter is the state $|\psi_{out}\rangle_{34}$ not presented here explicitly. The parameter δ defines the range in which the misfit parameter ε is assumed to be smaller than a prescribed value. As the misfit parameter changes with the measurement results within the measurement ranges, the accuracy of the preparation can be characterized by the average misfit defined as $\varepsilon_{\text{avg}} = \sum_j \varepsilon_j P_j / \sum_j P_j$, where the misfits ε_j and the probabilities P_j are calculated for appropriately small subranges of the whole measurement range [16].

III. GENERATION OF NONCLASSICAL STATES

In the following, we demonstrate through examples that the proposed scheme is capable of generating a wide variety of nonclassical states with high performance. Our examples include binomial states $|p, M\rangle_B$ [23], negative binomial states

$|\eta, M, \varphi\rangle_{NB}$ [24], and amplitude squeezed states $|\alpha_0, u, \delta\rangle_{AS}$ [25], having the following photon number expansions:

$$|p, M\rangle_B = \sum_{n=0}^M \left[\binom{M}{n} p^n (1-p)^{M-n} \right]^{\frac{1}{2}} |n\rangle, \quad (4)$$

$$|\eta, M, \varphi\rangle_{NB} = \mathcal{N} \sum_{n=0}^{\infty} \binom{M+n-1}{n}^{\frac{1}{2}} (\eta e^{i\varphi})^n |n\rangle, \quad (5)$$

$$|\alpha_0, u, \delta\rangle_{AS} = \mathcal{N} \sum_{n=0}^{\infty} \frac{\sqrt{2\pi}\alpha_0^n}{u\sqrt{n!}} \exp\left[-\frac{(\delta-n)^2}{2u^2}\right] |n\rangle. \quad (6)$$

For $0 < p < 1$ the binomial state is the superposition of the first $M+1$ photon number states. Binomial states can be used, e.g., for measuring the canonical phase of the quantum electromagnetic field states [26] or they can be applied as optimal input states for communication purposes in a non-Gaussian quantum channel [27]. Negative binomial states reduce to the Susskind-Glogower phase states for $M = 1$ [24,28]. Amplitude squeezed states contract into the coherent state $|\alpha_0\rangle$ in the limit $u \rightarrow \infty$, while in the opposite limit $u \ll 1$, an n -photon number state with $n = \delta$ is achieved. Amplitude squeezed states are intelligent states of the Pegg-Barnett number-phase uncertainty relation and also of an alternative to this relation introduced as the number-operator-annihilation

operator uncertainty relation for a certain parameter range [25,29,30]. Hence, they can be used for testing various uncertainty relations experimentally [31,32].

We also consider superpositions of photon number states with *ad hoc* coefficients and the special superposition

$$|\psi(\zeta, \chi')\rangle_{\text{RS}} = \hat{S}(\zeta) \left(|0\rangle + \chi' \frac{3}{2\sqrt{2}} |1\rangle + \chi' \frac{\sqrt{3}}{2} |3\rangle \right) \quad (7)$$

referred to as resource states that can be used for realizing cubic nonlinear quantum gates essential for universal continuous-variable quantum computation in the optical setting [22,33,34]. Finally, we present results on the generation of squeezed cat states $|\alpha, r, \theta\rangle_{\text{SC}\pm} = \mathcal{N}\hat{S}(\zeta)(|\alpha\rangle \pm |\alpha\rangle)$, squeezed number states $|n, r, \theta\rangle_{\text{Sn}} = \hat{S}(\zeta)|n\rangle$, and displaced squeezed number states $|n, r, \theta\rangle_{\text{DSn}} = \hat{D}(\alpha)|n, r, \theta\rangle_{\text{Sn}}$ for $n = 1, 2, 3$. These states can be used efficiently in optical quantum metrology for high-precision phase measurement in the low-photon-number regime [35–37]. Squeezed cat states with zero squeezing, i.e., the even and odd cat states, form a basis for linear optical quantum computing [38,39].

To generate a given target state, our task is to find the values of the variable parameters of the introduced scheme for which the misfit between the target and the generated states is minimal. (Another valid goal would be the simultaneous optimization of the probability and the misfit. We opt for minimizing the misfit, though we shall comment on the other option as well later.) Analyzing the target function of the optimization, we have found that the optimization problem is neither linear nor convex. Therefore, we have used a genetic algorithm [40,41] to solve this optimization problem. We have imposed bounds on the variables so that their values are physically reasonable while the optimization problem is numerically stable and feasible. The applied ranges are $0 \leq r_i \leq 1.7$, $0 \leq \alpha_i \leq 4$, $0.1 \leq T \leq 0.9$, $0 \leq x \leq 4$, and all the phase angles θ_i , ϕ_i , and λ are allowed to take any possible values between 0 and 2π . In the genetic algorithm used for our calculations, we set the options of the optimization such as the population, the number of generations, and the function tolerance in such a way that the optimization is stable and the results are reproducible.

In Table I we present the result of the optimization for binomial states, negative binomial states, amplitude squeezed states, resource states, and various number state superpositions for the HM and single-photon detection (SPD) versions of the scheme. In the table, the range δ of the homodyne measurement has been chosen to keep the average misfit ε_{avg} below 10^{-2} . We note that increasing the parameter δ increases the success probability while the fidelity decreases. Table II contains the results of the optimization for number states, squeezed number states, displaced squeezed number states, amplitude squeezed states, and resource states for the MPD version of the scheme. Finally, results of the optimization for the cat and squeezed cat states are shown in Table III for the MPD version of the scheme.

The examples demonstrate that all the considered states can be generated with high fidelities, i.e., low misfits, using the proposed conditional scheme. The achievable success probabilities of the generation can be considered as high, as compared to those that can be typically achieved in other

quantum state engineering methods [8,9,16]. From the results presented in Table I, one can conclude that binomial states and negative binomial states can be generated with similar fidelity by using either the SPD or the HM version of the proposed scheme. In the case of amplitude squeezed states, the scheme yields higher fidelity with HM for low squeezing ($u \gg 1$) and with SPD for high squeezing ($u \lesssim 1$), respectively. All the other states can be generated by the proposed scheme with higher fidelity using SPD than HM. Generally, the states close to a Gaussian state can be generated by the scheme with HM, while the scheme containing SPD can be applied for the generation of states having a significantly non-Gaussian character. The results also show that certain nonclassical states can be approximated by Gaussian states with high fidelity.

The results in Table II show that number states, squeezed number states, and displaced squeezed number states can be generated in this scheme with almost negligible misfit, that is, with very high fidelity. Number states can be generated by interfering orthogonally squeezed vacuum states with identical real squeezing parameters and using a PNRD that, in case of success, detects the number of photons, which is equal to the photon number of the target state. Recall that the phase shift necessary for the orthogonal squeezing at the beam splitter is already included in the scheme, therefore the squeezing angles θ_1 and θ_2 in Table II are equal. We have observed that this common value of these angles has no effect on the result; we have fixed this value to be π , which is an arbitrary choice. The results on the generation of number states supports a simple intuitive explanation. The two-mode output state of the scheme containing a beam splitter of transmittance $T = 0.5$ with the chosen inputs is a two-mode squeezed state. Thus the detection of a given photon number in one of the modes results in the generation of the same photon number state in the other mode. This physical process is well known and it is exploited in single-photon generation schemes based on spontaneous parametric down-conversion [42–46]. For the optimal generation of squeezed number and displaced squeezed number states, the aforementioned matching of the detected photon number with that of the target state still applies. Squeezed number states with $N = 2$ and 3 can be generated by interfering orthogonally squeezed vacuum states with different squeezing parameters. The squeezing angle of one of the input states is equal to the squeezing angle of the given state. For generating displaced squeezed number states, special squeezed coherent state inputs are needed.

At the end of Table II we present results for amplitude squeezed states and resource states generated by the scheme containing MPD. We have found that for the amplitude squeezed states with high squeezing ($u \lesssim 1$), when the state tends to approximate the n -photon number state with $n = \delta$, the MPD with matching n gives the best result again. For comparison, we present the results of the optimization for the amplitude squeezed state $|\sqrt{3}, 1, 3\rangle_{\text{AS}}$ for the cases $n = 3$ (matching case) and $n = 1$. In contrast, in the case of resource states that do not have a characteristic photon number, the scheme with MPD gives results similar to those with SPD.

Table III presents results for cat states and squeezed cat states. The data show that cat states with zero squeezing can be generated by using orthogonally squeezed vacuum states with special real squeezing parameters, while squeezed cat

TABLE I. Results of the optimization for generating binomial, negative binomial, amplitude squeezed, and resource states, and special photon number superpositions in the scheme of Fig. 1 with HM and SPD. The table presents for each state the minimal misfit ε and the corresponding optimal choice of parameters: the parameters of the input squeezed coherent states ($r_1, \theta_1, \alpha_1, \phi_1, r_2, \theta_2, \alpha_2$, and ϕ_2), the transmittance of the beam splitter T , and the success probability P . For the HM-based version of the scheme, the table also contains the measurement result x of the rotated quadrature operator X_λ rotated by the angle λ , the range δ of the measurement, and the average misfit ε_{avg} . Parameters denoted by bold characters are fixed.

State	ε	r_1	θ_1	α_1	ϕ_1	r_2	θ_2	α_2	ϕ_2	T	x	λ	δ	P	ε_{avg}
$ 0.3, 7\rangle_B$	1.14×10^{-4}	0.60	3.90	1.00	4.26	0.75	3.62	0.70	0.48	0.59	0.60	2.17	0.17	0.125	0.008
$ 0.3, 7\rangle_B$	1.26×10^{-4}	0.74	3.50	0.10	2.14	0.16	4.43	1.97	0.08	0.69				0.318	
$ 0.45, 8\rangle_B$	8.06×10^{-4}	0.45	0.74	0.34	1.01	0.45	0.28	1.97	0.06	0.90	0.61	0.04	0.30	0.275	0.008
$ 0.45, 8\rangle_B$	8.15×10^{-4}	0.51	3.22	2.44	4.95	0.22	6.18	0.54	5.58	0.65				0.079	
$ 0.2, 10\rangle_B$	1.66×10^{-5}	0.60	1.95	1.00	4.77	0.75	2.86	0.70	6.10	0.49	0.25	0.56	0.17	0.132	0.009
$ 0.2, 10\rangle_B$	1.88×10^{-5}	0.16	3.39	0.49	4.70	0.09	5.68	1.51	6.27	0.47				0.369	
$ 0.4, 15\rangle_B$	1.91×10^{-4}	1.54	1.08	0.93	3.06	0.27	0.28	2.36	0.09	0.90	0.73	2.57	0.30	0.527	0.003
$ 0.65, 1, 0\rangle_{NB}$	7.83×10^{-4}	0.62	0.13	0.09	0.25	0.21	0.90	0.98	0.02	0.70	0.23	0.03	0.20	0.265	0.008
$ \frac{0.5, 5}{4}, \frac{\pi}{4}\rangle_{NB}$	3.36×10^{-5}	0.56	0.72	0.58	0.34	0.10	0.07	1.34	0.59	0.80	0.24	0.03	0.30	0.362	0.006
$ \frac{0.5, 5}{4}, \frac{\pi}{4}\rangle_{NB}$	3.37×10^{-5}	0.60	1.57	0.80	3.14	0.60	2.36	2.47	0.69	0.63	1.55	3.79	0.18	0.065	0.008
$ \frac{0.5, 5}{4}, \frac{\pi}{4}\rangle_{NB}$	3.40×10^{-5}	0.06	1.17	2.11	5.44	0.19	4.78	0.08	3.16	0.65				0.159	
$ \frac{0.75, 6}{2}, \frac{\pi}{2}\rangle_{NB}$	3.53×10^{-4}	0.60	1.57	0.80	3.14	0.60	0.46	3.04	1.53	0.86	2.60	3.67	0.23	0.146	0.009
$ \frac{0.75, 6}{2}, \frac{\pi}{2}\rangle_{NB}$	4.96×10^{-4}	0.43	2.45	0.12	5.57	0.45	0.32	3.21	1.63	0.72				0.200	
$ 0.45, 10, 0\rangle_{NB}$	8.84×10^{-6}	0.60	6.14	1.00	4.44	0.75	4.98	0.70	5.57	0.58	0.76	3.27	0.16	0.080	0.008
$ 0.45, 10, 0\rangle_{NB}$	9.15×10^{-6}	0.08	5.54	0.07	2.35	0.12	3.23	1.69	0.00	0.88				0.246	
$ 1, 0.5, 1\rangle_{AS}$	2.45×10^{-7}	0.60	2.32	0.09	5.89	0.60	2.30	0.20	5.86	0.50				0.210	
$ 1, 0.5, 1\rangle_{AS}$	2.40×10^{-7}	0.37	0.68	0.14	5.02	0.71	0.67	0.09	4.98	0.37				0.167	
$ 1, 1, 1\rangle_{AS}$	2.07×10^{-4}	0.45	1.05	0.76	5.22	0.50	0.86	0.42	5.18	0.51				0.258	
$ 1, 1, 1\rangle_{AS}$	2.21×10^{-4}	0.60	3.91	0.48	3.51	0.60	4.06	1.06	0.46	0.47				0.270	
$ 1, 2, 1\rangle_{AS}$	1.22×10^{-3}	0.37	1.61	1.29	2.40	0.23	0.86	1.78	0.36	0.70	1.71	3.10	0.40	0.366	0.007
$ 1, 2, 1\rangle_{AS}$	1.18×10^{-3}	0.26	4.08	0.12	2.74	0.34	5.53	1.44	0.16	0.47				0.378	
$ \sqrt{3}, 5, 3\rangle_{AS}$	5.78×10^{-5}	0.60	5.14	1.00	4.53	0.75	4.61	0.70	4.72	0.68	0.79	2.83	0.16	0.097	0.008
$ \sqrt{3}, 5, 3\rangle_{AS}$	1.65×10^{-4}	0.56	3.81	0.02	3.15	0.17	4.64	2.05	0.07	0.74				0.389	
$ 1, 6, 1\rangle_{AS}$	7.25×10^{-7}	0.60	2.49	1.00	4.22	0.75	3.09	0.70	0.47	0.70	0.87	4.25	0.17	0.081	0.009
$ 1, 6, 1\rangle_{AS}$	1.49×10^{-4}	0.36	2.12	0.40	2.53	0.35	1.63	1.67	6.28	0.50				0.271	
$ \Psi(0.6, 0.03)\rangle_{RS}$	6.69×10^{-4}	0.46	2.99	0.07	6.26	1.15	0.28	0.02	1.35	0.30	0.23	6.13	0.55	0.222	0.006
$ \Psi(0.6, 0.03)\rangle_{RS}$	2.85×10^{-4}	1.02	2.70	0.76	5.27	0.61	0.23	0.36	4.02	0.79				0.329	
$ \Psi(0.15, 0.1)\rangle_{RS}$	7.28×10^{-3}	0.89	3.31	0.89	3.44	0.03	5.52	0.09	1.63	0.75	0.00	3.19	0.30	0.122	0.009
$ \Psi(0.15, 0.1)\rangle_{RS}$	1.80×10^{-3}	1.35	2.78	0.85	0.3	0.11	2.81	0.11	3.77	0.89				0.165	
$ \Psi(0.1i, 0.15)\rangle_{RS}$	4.32×10^{-3}	0.36	1.64	0.58	0.60	0.55	2.30	0.45	5.23	0.62				0.314	
$ \Psi(0.1i, 0.15)\rangle_{RS}$	4.74×10^{-3}	0.60	0.92	0.77	5.83	0.60	1.79	0.53	4.56	0.59				0.318	
$ \Psi(0.4, 0.166)\rangle_{RS}$	5.31×10^{-3}	0.54	5.66	1.34	4.31	1.17	5.93	1.31	1.85	0.50				0.148	
$ \Psi(0.4, 0.166)\rangle_{RS}$	5.37×10^{-3}	0.60	1.72	1.14	5.86	0.60	1.00	0.96	4.78	0.54				0.209	
$\frac{1}{\sqrt{2}}(0\rangle + 1\rangle)$	1.40×10^{-6}	0.41	2.52	0.25	0.63	0.61	2.52	0.74	5.88	0.41				0.236	
$\frac{1}{\sqrt{2}}(0\rangle + 1\rangle)$	5.70×10^{-6}	0.60	0.00	0.82	4.71	0.60	6.28	0.25	3.16	0.50				0.274	
$\frac{1}{\sqrt{5}}(2 1\rangle + 2\rangle)$	2.74×10^{-3}	0.35	6.05	0.41	4.66	1.39	6.13	0.21	0.95	0.35				0.159	
$\frac{1}{\sqrt{17}}(4 1\rangle + 3\rangle)$	2.68×10^{-3}	0.71	5.16	0.01	1.00	0.79	4.56	0.00	0.74	0.46				0.229	
$\frac{1}{\sqrt{17}}(4 1\rangle + 3\rangle)$	2.69×10^{-3}	0.60	1.85	0.00	4.86	0.60	2.44	0.00	2.79	0.60				0.190	
$\frac{1}{3}(2 0\rangle + 2 1\rangle + 2\rangle)$	3.36×10^{-3}	0.19	5.74	0.76	4.58	0.27	6.23	0.22	0.45	0.72				0.207	
$\mathcal{N}(1\rangle + 0.3 3\rangle + 0.1 5\rangle)$	7.36×10^{-4}	1.08	0.00	0.00	0.00	0.12	0.00	0.00	0.00	0.60				0.131	

states can be produced at general squeezed vacuum input with special squeezing parameters and angles. Even cat states can be generated by using $n = 2$, while detecting an odd number of photons, that is, $n = 1$ or 3, makes possible the generation

of odd cat states. For a given detected photon number n , by increasing the coherent amplitude α of the cat and the squeezed cat states, the misfit increases. Comparing results for the same states and different detected photon numbers n , it

TABLE II. Results of the optimization for generating number, squeezed and displaced squeezed number, amplitude squeezed, and resource states in the scheme of Fig. 1 with MPD. The table presents for each state the minimal misfit ε and the corresponding optimal choice of parameters: the parameters of the input squeezed coherent states ($r_1, \theta_1, \alpha_1, \phi_1, r_2, \theta_2, \alpha_2$, and ϕ_2), the transmittance of the beam splitter T , the detected photon number n , and the success probability P . Parameters denoted by bold characters are fixed.

State	ε	r_1	θ_1	α_1	ϕ_1	r_2	θ_2	α_2	ϕ_2	T	n	P
$ 1, 0, 0\rangle_{S1}$	1.80×10^{-14}	0.88	3.14	0.00	0.00	0.88	3.14	0.00	0.00	0.50	1	0.250
$ 1, 0.2, 0\rangle_{S1}$	2.02×10^{-14}	0.80	0.00	0.00	0.00	0.90	0.00	0.00	0.00	0.62	1	0.247
$ 1, 0.3, 1.571\rangle_{S1}$	9.66×10^{-8}	0.60	3.60	0.00	0.00	0.60	2.46	0.00	0.00	0.54	1	0.165
$ 1, 0.4, 0\rangle_{S1}$	1.63×10^{-13}	0.91	0.00	0.00	0.00	0.65	0.00	0.00	0.00	0.85	1	0.151
$ 1, 0.4, 2.356\rangle_{S1}$	3.18×10^{-7}	0.60	3.07	0.00	0.00	0.60	2.48	0.00	0.00	0.84	1	0.129
$ 1, 0.6, 1.571\rangle_{S1}$	1.03×10^{-9}	0.77	1.57	0.00	0.00	1.01	1.57	0.00	0.00	0.84	1	0.222
$ 2, 0, 0\rangle_{S2}$	3.17×10^{-10}	1.15	3.14	0.00	0.00	1.15	3.14	0.00	0.00	0.50	2	0.148
$ 2, 0.3, 0\rangle_{S2}$	1.81×10^{-6}	1.38	3.14	0.00	0.00	1.08	3.14	0.00	0.00	0.35	2	0.147
$ 2, 0.4, 0\rangle_{S2}$	5.56×10^{-6}	1.01	0.00	0.00	0.00	1.41	0.00	0.00	0.00	0.69	2	0.148
$ 2, 0.6, 0\rangle_{S2}$	5.50×10^{-5}	0.89	0.00	0.00	0.00	1.48	0.00	0.00	0.00	0.77	2	0.147
$ 2, 0.7, 0.785\rangle_{S2}$	7.48×10^{-8}	0.42	0.79	0.00	0.00	1.12	0.79	0.00	0.00	0.83	2	0.069
$ 3, 0, 0\rangle_{S3}$	3.88×10^{-7}	1.32	3.14	0.00	0.00	1.32	3.14	0.00	0.00	0.50	3	0.105
$ 3, 0.2, 0\rangle_{S3}$	3.12×10^{-9}	1.06	3.14	0.00	0.00	0.86	3.14	0.00	0.00	0.40	3	0.074
$ 3, 0.3, 0\rangle_{S3}$	6.82×10^{-8}	0.90	0.00	0.00	0.00	1.20	0.00	0.00	0.00	0.65	3	0.086
$ 3, 0.3, 2.356\rangle_{S3}$	1.25×10^{-7}	1.22	5.50	0.00	0.00	0.92	5.50	0.00	0.00	0.35	3	0.089
$ 3, 0.4, 0\rangle_{S3}$	1.19×10^{-8}	1.11	3.14	0.00	0.00	0.71	3.14	0.00	0.00	0.30	3	0.060
$ 3, 0.5, 0\rangle_{S3}$	2.52×10^{-7}	1.19	3.14	0.00	0.00	0.69	3.14	0.00	0.00	0.26	3	0.061
$ 3, 0.6, 1.571\rangle_{S3}$	6.26×10^{-6}	1.30	4.71	0.00	0.00	0.70	4.71	0.00	0.00	0.22	3	0.067
$ 1, 0.3, 0, 0.5\rangle_{DS1}$	7.96×10^{-5}	1.90	1.76	0.26	4.28	1.09	1.09	0.37	0.03	0.57	1	0.135
$ 1, 0.3, 0, 1\rangle_{DS1}$	3.49×10^{-5}	1.71	1.43	0.70	4.78	1.40	0.84	0.77	6.27	0.59	1	0.138
$ 1, 0.6, 3.14, 0.5i\rangle_{DS1}$	4.51×10^{-5}	1.41	0.73	0.40	6.21	1.94	1.94	0.31	1.55	0.40	1	0.119
$ 1, 0.4, 0, 1.5\rangle_{DS1}$	3.56×10^{-5}	1.37	2.56	1.21	4.71	1.83	1.87	0.82	0.06	0.35	1	0.127
$ 2, 0.3, 1.571, 1.2\rangle_{DS2}$	2.10×10^{-5}	1.07	4.71	0.71	4.71	1.37	4.71	0.97	0.00	0.65	2	0.147
$ 2, 0.3, 0.785, 1.2\rangle_{DS2}$	2.45×10^{-5}	1.45	3.93	0.97	4.71	1.14	3.93	0.72	0.00	0.35	2	0.144
$ 2, 0.1, 0, 1.4\rangle_{DS2}$	2.47×10^{-4}	1.47	0.92	1.03	4.72	1.42	1.11	0.97	6.27	0.47	2	0.128
$ 2, 0.6, 0, 1.65\rangle_{DS2}$	4.68×10^{-5}	0.75	3.15	0.78	4.71	1.35	3.15	1.45	0.00	0.78	2	0.137
$ 3, 0.2, 0, 0.75\rangle_{DS3}$	5.32×10^{-5}	1.17	3.24	0.47	4.71	1.37	3.20	0.58	0.00	0.60	3	0.105
$ 3, 0.3, 0, 1.8\rangle_{DS3}$	6.52×10^{-4}	1.32	0.32	1.08	4.71	1.58	0.17	1.45	0.00	0.64	3	0.103
$ 3, 0.45, 0, 1.35\rangle_{DS3}$	2.34×10^{-5}	0.85	3.14	0.72	4.71	1.30	3.14	1.14	6.28	0.72	3	0.086
$ \sqrt{2}, 0.2, 2\rangle_{AS}$	1.65×10^{-6}	1.41	6.21	0.00	0.00	1.41	6.21	0.00	0.00	0.50	2	0.133
$ \sqrt{2}, 0.5, 2\rangle_{AS}$	1.81×10^{-5}	1.18	3.64	0.15	3.35	1.16	3.65	0.55	0.25	0.50	2	0.148
$ \sqrt{2}, 1, 2\rangle_{AS}$	3.09×10^{-4}	0.74	0.01	1.42	4.71	0.95	6.28	0.02	3.79	0.50	2	0.175
$ \sqrt{3}, 0.2, 3\rangle_{AS}$	4.99×10^{-7}	1.33	2.15	0.00	0.00	1.33	2.15	0.00	0.00	0.50	3	0.106
$ \sqrt{3}, 0.5, 3\rangle_{AS}$	3.24×10^{-5}	0.95	3.73	0.09	3.44	0.93	3.73	0.30	0.29	0.50	3	0.075
$ \sqrt{3}, 1, 3\rangle_{AS}$	3.62×10^{-4}	1.13	3.16	0.02	2.32	0.91	3.16	1.77	0.01	0.50	3	0.126
$ \sqrt{3}, 1, 3\rangle_{AS}$	5.64×10^{-2}	1.48	2.90	0.81	5.60	0.14	0.54	1.10	6.22	0.75	1	0.091
$ \Psi(0.4, 0.166)\rangle_{RS}$	5.19×10^{-3}	0.10	2.95	0.06	5.78	1.82	0.18	1.25	4.16	0.09	2	0.069
$ \Psi(0.4, 0.166)\rangle_{RS}$	2.82×10^{-3}	0.66	0.55	1.15	5.23	0.65	0.47	1.05	3.65	0.54	3	0.150
$ \Psi(0.5, 0.2)\rangle_{RS}$	7.66×10^{-3}	0.13	0.02	0.28	4.72	0.52	6.28	0.37	3.15	0.65	1	0.218
$ \Psi(0.5, 0.2)\rangle_{RS}$	2.89×10^{-3}	0.33	2.08	0.59	0.10	0.81	0.24	0.38	4.92	0.42	2	0.107
$ \Psi(0.5, 0.2)\rangle_{RS}$	2.68×10^{-3}	0.38	3.98	0.66	2.69	1.04	5.89	0.98	0.93	0.27	3	0.090

can be deduced from the data that the increase in the number of detected photons n leads to the decrease of the minimal misfit, that is, to the improvement of the fidelity.

For comparison, we present data also for the generation of cat states in two experimentally realized special conditional

schemes known from the literature. (These are the rows below the horizontal line in Table III.) In one of these schemes, the mixing of a squeezed vacuum state with a vacuum state on a beam splitter was considered [4]. In the other scheme, two squeezed vacuum states with equal squeezing were mixed by

TABLE III. Results of the optimization for generating cat and squeezed cat states in the scheme of Fig. 1 with MPD. The table presents for each state the minimal misfit ε and the corresponding optimal choice of parameters: the parameters of the input squeezed coherent states (r_1 , θ_1 , α_1 , ϕ_1 , r_2 , θ_2 , α_2 , and ϕ_2), the transmittance of the beam splitter T , the detected photon number n , and the success probability P . Parameters denoted by bold characters are fixed. Below the line are the results of the optimization for a single squeezed vacuum state input ($r_2 = 0$) and for squeezed vacuum inputs with equal squeezing ($r_1 = r_2$).

State	ε	r_1	θ_1	α_1	ϕ_1	r_2	θ_2	α_2	ϕ_2	T	n	P
$ 0.6, 0, 0\rangle_{SC^-}$	6.01×10^{-5}	0.60	5.27	0.00	0.00	0.60	4.86	0.00	0.00	0.46	1	0.199
$ 0.6, 0.5, 1.571\rangle_{SC^-}$	6.01×10^{-5}	0.66	5.16	0.00	0.00	0.71	0.38	0.00	0.00	0.19	1	0.110
$ 0.7, 0, 0\rangle_{SC^-}$	2.00×10^{-4}	0.60	4.43	0.00	0.00	0.60	3.92	0.00	0.00	0.58	1	0.195
$ 0.7, 0.6, 0.7854\rangle_{SC^-}$	2.00×10^{-4}	0.19	3.78	0.00	0.00	0.84	1.05	0.00	0.00	0.58	1	0.069
$ 0.8, 0, 0\rangle_{SC^-}$	5.58×10^{-4}	1.18	3.14	0.00	0.00	1.24	3.14	0.00	0.00	0.62	1	0.211
$ 0.8, 0.5, 1.571\rangle_{SC^-}$	5.58×10^{-4}	0.14	0.40	0.00	0.00	0.72	1.85	0.00	0.00	0.82	1	0.074
$ 1, 0, 0\rangle_{SC^-}$	2.89×10^{-3}	1.11	0.00	0.00	0.00	0.20	0.00	0.00	0.00	0.50	1	0.169
$ 1, 0, 0\rangle_{SC^-}$	2.89×10^{-3}	0.54	3.14	0.00	0.00	1.14	3.14	0.00	0.00	0.61	1	0.238
$ 1, 0, 0\rangle_{SC^-}$	2.89×10^{-3}	0.60	0.91	0.00	0.00	0.60	2.10	0.00	0.00	0.48	1	0.162
$ 1, 0.5, 2.356\rangle_{SC^-}$	2.89×10^{-3}	0.22	0.64	0.00	0.00	1.14	2.50	0.00	0.00	0.77	1	0.137
$ 1.2, 0, 0\rangle_{SC^-}$	9.91×10^{-3}	0.94	0.00	0.00	0.00	0.60	0.00	0.00	0.00	0.26	1	0.233
$ 1.4, 0, 0\rangle_{SC^-}$	2.50×10^{-2}	1.00	3.14	0.00	0.00	1.08	3.14	0.00	0.00	0.81	1	0.226
$ 1.4, 0, 0\rangle_{SC^-}$	2.50×10^{-2}	0.68	0.00	0.00	0.00	0.42	0.00	0.00	0.00	0.10	1	0.100
$ 0.8, 0, 0\rangle_{SC^+}$	8.57×10^{-6}	0.10	3.14	0.00	0.00	0.88	3.14	0.00	0.00	0.27	2	0.103
$ 1, 0, 0\rangle_{SC^+}$	9.79×10^{-5}	0.15	3.14	0.00	0.00	1.82	3.14	0.00	0.00	0.30	2	0.092
$ 1.1, 0.45, 0.785\rangle_{SC^+}$	2.61×10^{-4}	1.61	5.40	0.00	0.00	0.44	0.37	0.00	0.00	0.72	2	0.103
$ 1.2, 0, 0\rangle_{SC^+}$	6.08×10^{-4}	0.19	3.14	0.00	0.00	1.48	3.14	0.00	0.00	0.40	2	0.105
$ 1.4, 0, 0\rangle_{SC^+}$	2.42×10^{-3}	0.19	3.14	0.00	0.00	1.15	3.14	0.00	0.00	0.51	2	0.095
$ 1.4, 0.75, 2.094\rangle_{SC^+}$	2.45×10^{-3}	0.15	4.02	0.00	0.00	1.42	2.30	0.00	0.00	0.85	2	0.098
$ 1.6, 0, 0\rangle_{SC^+}$	6.93×10^{-3}	0.22	3.14	0.00	0.00	1.35	3.14	0.00	0.00	0.56	2	0.103
$ 0.8, 0, 0\rangle_{SC^-}$	4.63×10^{-7}	0.10	3.14	0.00	0.00	1.00	3.14	0.00	0.00	0.20	3	0.043
$ 1, 0, 0\rangle_{SC^-}$	6.42×10^{-6}	0.14	3.14	0.00	0.00	1.50	3.14	0.00	0.00	0.25	3	0.063
$ 1.1, 0.45, 0.785\rangle_{SC^-}$	1.83×10^{-5}	1.07	5.19	0.00	0.00	0.44	0.37	0.00	0.00	0.72	3	0.055
$ 1.2, 0, 0\rangle_{SC^-}$	4.81×10^{-5}	0.15	3.14	0.00	0.00	0.80	3.14	0.00	0.00	0.40	3	0.028
$ 1.2, 0.5, 1.571\rangle_{SC^-}$	4.81×10^{-5}	1.56	5.35	0.00	0.00	0.34	0.88	0.00	0.00	0.54	3	0.067
$ 1.3, 0.8, 0.785\rangle_{SC^-}$	1.14×10^{-4}	1.39	4.59	0.00	0.00	0.65	0.26	0.00	0.00	0.54	3	0.068
$ 1.4, 0, 0\rangle_{SC^-}$	2.48×10^{-4}	0.22	3.14	0.00	0.00	1.63	3.14	0.00	0.00	0.39	3	0.071
$ 1.6, 0, 0\rangle_{SC^-}$	9.23×10^{-4}	0.23	3.14	0.00	0.00	1.23	3.14	0.00	0.00	0.48	3	0.061
$ 1.8, 0, 0\rangle_{SC^-}$	2.68×10^{-3}	0.28	3.14	0.00	0.00	1.86	3.14	0.00	0.00	0.51	3	0.071
$ 2, 0, 0\rangle_{SC^-}$	6.22×10^{-3}	0.28	3.14	0.00	0.00	1.46	3.14	0.00	0.00	0.58	3	0.070
$ 0.8, 0, 0\rangle_{SC^-}$	5.58×10^{-4}	0.43	0.00	0.00	0.00	0.00	0.00	0.00	0.00	0.50	1	0.040
$ 0.8, 0, 0\rangle_{SC^-}$	5.58×10^{-4}	0.91	0.00	0.00	0.00	0.91	0.00	0.00	0.00	0.36	1	0.119
$ 1, 0, 0\rangle_{SC^-}$	2.89×10^{-3}	0.45	0.00	0.00	0.00	0.00	0.00	0.00	0.00	0.28	1	0.038
$ 1, 0, 0\rangle_{SC^-}$	2.89×10^{-3}	0.80	0.00	0.00	0.00	0.80	0.00	0.00	0.00	0.27	1	0.097
$ 1.2, 0, 0\rangle_{SC^-}$	9.91×10^{-3}	1.23	0.00	0.00	0.00	0.00	0.00	0.00	0.00	0.52	1	0.124
$ 1.2, 0, 0\rangle_{SC^-}$	9.91×10^{-3}	0.73	0.00	0.00	0.00	0.73	0.00	0.00	0.00	0.18	1	0.071
$ 1.4, 0, 0\rangle_{SC^-}$	2.50×10^{-2}	0.84	0.00	0.00	0.00	0.00	0.00	0.00	0.00	0.28	1	0.105
$ 1.4, 0, 0\rangle_{SC^-}$	2.50×10^{-2}	1.12	0.00	0.00	0.00	1.12	0.00	0.00	0.00	0.19	1	0.138
$ 0.8, 0, 0\rangle_{SC^-}$	2.04×10^{-4}	1.93	0.00	0.00	0.00	0.00	0.00	0.00	0.00	0.87	3	0.033
$ 0.8, 0, 0\rangle_{SC^-}$	1.27×10^{-4}	0.40	3.14	0.00	0.00	0.40	3.14	0.00	0.00	0.91	3	0.002
$ 1, 0, 0\rangle_{SC^-}$	1.08×10^{-3}	2.00	0.00	0.00	0.00	0.00	0.00	0.00	0.00	0.80	3	0.041
$ 1, 0, 0\rangle_{SC^-}$	1.18×10^{-3}	0.58	3.14	0.00	0.00	0.58	3.14	0.00	0.00	0.92	3	0.006
$ 1.2, 0, 0\rangle_{SC^-}$	3.85×10^{-3}	2.00	0.00	0.00	0.00	0.00	0.00	0.00	0.00	0.73	3	0.048
$ 1.2, 0, 0\rangle_{SC^-}$	5.64×10^{-3}	0.75	3.14	0.00	0.00	0.75	3.14	0.00	0.00	0.93	3	0.011
$ 1.4, 0, 0\rangle_{SC^-}$	1.01×10^{-2}	2.00	0.00	0.00	0.00	0.00	0.00	0.00	0.00	0.65	3	0.054
$ 1.4, 0, 0\rangle_{SC^-}$	1.72×10^{-2}	0.91	3.14	0.00	0.00	0.91	3.14	0.00	0.00	0.94	3	0.014

TABLE IV. Examples from the Pareto optimal sets of the multiobjective optimization for generating resource states and cat states in the scheme of Fig. 1 with MPD. In the optimization, both the misfit ε and the success probability P were used simultaneously as objective functions. The table presents for each state the minimal misfit ε and the corresponding optimal choice of parameters: the parameters of the input squeezed coherent states ($r_1, \theta_1, \alpha_1, \phi_1, r_2, \theta_2, \alpha_2$, and ϕ_2), the transmittance of the beam splitter T , the detected photon number n , and the success probability P .

State	ε	r_1	θ_1	α_1	ϕ_1	r_2	θ_2	α_2	ϕ_2	T	n	P
$ \Psi(0.4, 0.166)\rangle_{\text{RS}}$	5.31×10^{-3}	0.54	5.66	1.34	4.31	1.17	5.93	1.31	1.85	0.50	1	0.148
$ \Psi(0.4, 0.166)\rangle_{\text{RS}}$	5.34×10^{-3}	0.40	4.94	0.69	3.73	0.63	5.61	0.73	1.89	0.51	1	0.279
$ \Psi(0.4, 0.166)\rangle_{\text{RS}}$	8.74×10^{-3}	0.40	5.11	0.69	3.83	0.63	5.53	0.70	1.95	0.49	1	0.295
$ \Psi(0.4, 0.166)\rangle_{\text{RS}}$	1.09×10^{-2}	0.84	3.45	0.62	4.56	0.61	5.05	0.54	2.83	0.42	1	0.347
$ 0.8, 0, 0\rangle_{\text{SC-}}$	4.63×10^{-7}	0.10	3.14	0.00	0.00	1.00	3.14	0.00	0.00	0.20	3	0.043
$ 0.8, 0, 0\rangle_{\text{SC-}}$	3.11×10^{-6}	0.11	3.13	0.00	0.00	1.53	3.14	0.00	0.00	0.18	3	0.053
$ 0.8, 0, 0\rangle_{\text{SC-}}$	3.16×10^{-4}	0.18	3.14	0.00	0.00	1.49	3.14	0.00	0.00	0.20	3	0.060
$ 0.8, 0, 0\rangle_{\text{SC-}}$	8.98×10^{-3}	0.38	3.15	0.00	0.00	1.40	3.16	0.00	0.00	0.23	3	0.070
$ 1.2, 0, 0\rangle_{\text{SC-}}$	4.81×10^{-5}	0.15	3.14	0.00	0.00	0.80	3.14	0.00	0.00	0.40	3	0.028
$ 1.2, 0, 0\rangle_{\text{SC-}}$	4.81×10^{-5}	0.18	3.14	0.00	0.00	1.55	3.14	0.00	0.00	0.32	3	0.068
$ 1.2, 0, 0\rangle_{\text{SC-}}$	8.96×10^{-4}	0.24	3.14	0.00	0.00	1.50	3.14	0.00	0.00	0.33	3	0.070
$ 1.2, 0, 0\rangle_{\text{SC-}}$	5.05×10^{-3}	0.29	3.14	0.00	0.00	1.50	3.15	0.00	0.00	0.35	3	0.072

a beam splitter [6]. The presented results were obtained by using our optimization procedure along with the restrictions $r_2 = 0$ and $r_1 = r_2$ for the first and second schemes, respectively. The results show that in the case of single photon detection ($n = 1$), similar misfits can be achieved by using any of the three schemes, but our scheme containing two general squeezed vacuum states as inputs provides higher success probabilities. Comparing the results for three-photon detection ($n = 3$), it can be deduced that our scheme gives lower misfits, that is, higher fidelities, along with higher success probabilities.

As our aim was to generate the target states with the highest fidelity in our scheme, we chose the misfit parameter as the only objective function in the genetic algorithm in all the previous calculations. Naturally, it is possible to perform a multiobjective optimization (also called Pareto optimization) where both the misfit ε and the success probability P are used as objective functions of the genetic algorithm. In Table IV we present examples for the Pareto optimal sets of the multiobjective optimizations for some target states. As expected, higher probabilities in the found Pareto sets correspond to a decreased fidelity.

An interesting aspect of the proposed scheme is that some of the input parameters can be chosen freely in certain ranges without the significant deterioration of the fidelity. We checked this effect for the SPD and the HM version of the scheme. The number, type, and ranges of such parameters can differ for different target states. The number of the fixable parameters is obviously smaller for the scheme with SPD than for the one with HM due to the smaller number of adjustable parameters. We show some examples of states in which four or five parameters of the input states are fixed for the scheme with HM in Table I and two for the one with SPD in Tables I–III. In these examples, the fixed parameters are chosen in an *ad hoc* manner in the ranges $0.3 \leq r_1, r_2, \alpha_1, \alpha_2 \leq 1$ and $0 \leq \theta_1, \phi_1 \leq \pi$ for the binomial, negative binomial, and amplitude squeezed states, and $0.4 \leq r_1, r_2, \alpha_1, \alpha_2 \leq 0.8$ for all the other states. The possibility of using an input source

of fixed parameters is especially advantageous from an experimental point of view for it allows the generation of various states with high fidelity using the proposed scheme without relevant modification of the parametric setups generating the input states.

This feature is of particular importance, especially in the case of the scheme with HM. Those nonclassical states that can be approximated by Gaussian states according to the results in Table I can of course also be generated deterministically by producing directly the approximating Gaussian states. The parameters of these Gaussian states can be determined by using algorithms similar to the one applied in our approach. Note, however, that for direct generation of the approximating state, a different special setup is needed for each target state, while the setup with HM makes it possible to generate various nonclassical states with fixed inputs, that is, using the same setup generating the input states.

We note that most of the states presented in Tables I and III contain higher photon-number states ($n > 5$) with non-negligible coefficients in their photon-number expansion, except for the *ad hoc* photon-number state superpositions in Table I and the number states in Table II. Therefore, these states cannot be generated realistically by quantum state engineering methods based on repeated photon addition or subtraction. Most of the considered states can also be generated with the quantum state engineering methods based on coherent-state superpositions presented in Ref. [16], with a significantly lower success probability, however. It is important to remark that the method can be suitable for generating many more states than the examples presented here. Of course in the case of certain states for which specialized methods are also available, the general scheme may not outperform the special one.

Finally, we have considered the sensitivity of the method to the precision of the parameters of the input states and to the nonunit quantum efficiency of the measurements for the HM and the SPD versions of the scheme. The latter inefficiency can be represented by inserting an absorber in the signal beam

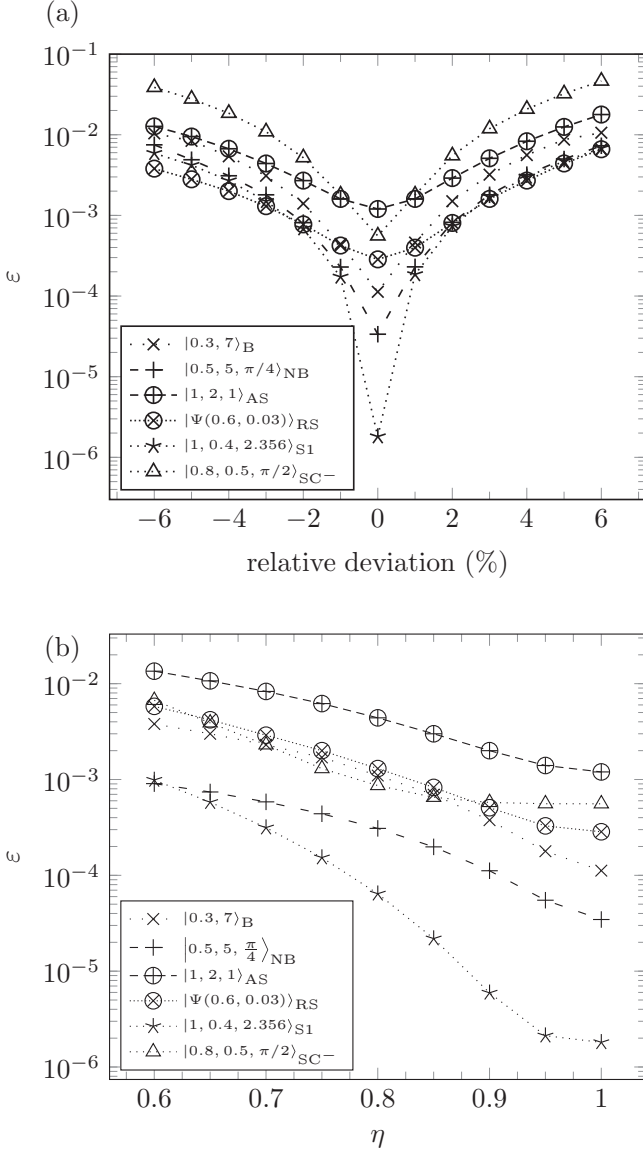


FIG. 2. Misfit as a function of (a) relative deviation of the parameters of the input states from their optimal value, and (b) detector efficiency η for some target states. Binomial and negative binomial states are generated with the scheme containing HM, while amplitude squeezed, squeezed number, squeezed cat, and resource states are generated with the scheme containing SPD.

path, which in turn can be modeled by a fictitious beam splitter with the signal beam entering one port and the vacuum state entering the other [47–50]. The transmittance of the beam splitter must be chosen to be equal to the quantum efficiency η . Note that such a model can describe other optical losses, e.g., the absorption of the beam path, and in the case of HM various other imperfections [50].

Figure 2 shows the change of the misfit as a function of (a) the relative shift of the parameters from their optimal value, and (b) the detector efficiency η for different target states prepared with the two versions of the scheme. One can conclude that the sensitivity is moderate for both considered inefficiencies. Hence, the considered nonclassical states can be prepared with high fidelities, even using input states generated with a precision available with current experimental technology and applying realistic measurement devices.

IV. CONCLUSIONS

We have proposed a quantum state engineering scheme based on the interference of two separately prepared squeezed coherent states for the conditional generation of various types of nonclassical states. Our approach unifies the benefits of simple conditional preparation and general quantum engineering schemes. It contains a single measurement thereby maintaining a proper success probability. Furthermore, it supports a broad variety of target states via parameter optimization. It can thus provide high-fidelity experimental access to many states that have relevant applications in quantum optics and quantum information science, and which cannot be efficiently generated otherwise.

ACKNOWLEDGMENTS

This research was supported by the National Research, Development and Innovation Office, Hungary (Projects No. K124351 and No. 2017-1.2.1-NKP-2017-00001 HunQuTech). The project has also been supported by the European Union, co-financed by the European Social Fund (Grants No. EFOP-3.6.1-16-2016-00004 entitled by Comprehensive Development for Implementing Smart Specialization Strategies at the University of Pécs, and No. EFOP-3.6.2-16-2017-00005).

- [1] J. S. Neergaard-Nielsen, B. M. Nielsen, C. Hettich, K. Mølmer, and E. S. Polzik, *Phys. Rev. Lett.* **97**, 083604 (2006).
- [2] A. Ourjoumtsev, H. Jeong, R. Tualle-Brouri, and P. Grangier, *Nature (London)* **448**, 784 (2007).
- [3] H. Takahashi, K. Wakui, S. Suzuki, M. Takeoka, K. Hayasaka, A. Furusawa, and M. Sasaki, *Phys. Rev. Lett.* **101**, 233605 (2008).
- [4] T. Gerrits, S. Glancy, T. S. Clement, B. Calkins, A. E. Lita, A. J. Miller, A. L. Migdall, S. W. Nam, R. P. Mirin, and E. Knill, *Phys. Rev. A* **82**, 031802(R) (2010).
- [5] J. Etesse, M. Bouillard, B. Kanseri, and R. Tualle-Brouri, *Phys. Rev. Lett.* **114**, 193602 (2015).
- [6] K. Huang, H. Le Jeannic, J. Ruaudel, V. B. Verma, M. D. Shaw, F. Marsili, S. W. Nam, E. Wu, H. Zeng, Y.-C. Jeong, R. Filip, O. Morin, and J. Laurat, *Phys. Rev. Lett.* **115**, 023602 (2015).
- [7] S. Szabo, P. Adam, J. Janszky, and P. Domokos, *Phys. Rev. A* **53**, 2698 (1996).
- [8] M. Dakna, J. Clausen, L. Knöll, and D.-G. Welsch, *Phys. Rev. A* **59**, 1658 (1999).
- [9] J. Fiurášek, R. García-Patrón, and N. J. Cerf, *Phys. Rev. A* **72**, 033822 (2005).
- [10] C. C. Gerry and A. Benmoussa, *Phys. Rev. A* **73**, 063817 (2006).

- [11] E. Bimbard, N. Jain, A. MacRae, and A. I. Lvovsky, *Nat. Photon.* **4**, 243 (2010).
- [12] J. Sperling, W. Vogel, and G. S. Agarwal, *Phys. Rev. A* **89**, 043829 (2014).
- [13] P. Adam, E. Molnar, G. Mogyorosi, A. Varga, M. Mechler, and J. Janszky, *Phys. Scr.* **90**, 074021 (2015).
- [14] K. Huang, H. Le Jeannic, V. B. Verma, M. D. Shaw, F. Marsili, S. W. Nam, E. Wu, H. Zeng, O. Morin, and J. Laurat, *Phys. Rev. A* **93**, 013838 (2016).
- [15] S.-Y. Lee and H. Nha, *Phys. Rev. A* **82**, 053812 (2010).
- [16] E. Molnar, P. Adam, G. Mogyorosi, and M. Mechler, *Phys. Rev. A* **97**, 023818 (2018).
- [17] D. Fukuda, G. Fujii, T. Numata, K. Amemiya, A. Yoshizawa, H. Tsuchida, H. Fujino, H. Ishii, T. Itatani, S. Inoue, and T. Zama, *Opt. Express* **19**, 870 (2011).
- [18] M. Schmidt, M. von Helversen, M. López, F. Gericke, E. Schlottmann, T. Heindel, S. Kück, S. Reitzenstein, and J. Beyer, *J. Low Temp. Phys.* **193**, 1243 (2018).
- [19] W. J. Zhang, H. Li, L. X. You, J. Huang, Y. H. He, L. Zhang, X. Y. Liu, S. J. Chen, Z. Wang, and X. M. Xie, *IEEE Photon. J.* **8**, 1 (2016).
- [20] Y. He, X. Ding, Z.-E. Su, H.-L. Huang, J. Qin, C. Wang, S. Unsleber, C. Chen, H. Wang, Y.-M. He, X.-L. Wang, W.-J. Zhang, S.-J. Chen, C. Schneider, M. Kamp, L.-X. You, Z. Wang, S. Höfling, C.-Y. Lu, and J.-W. Pan, *Phys. Rev. Lett.* **118**, 190501 (2017).
- [21] N. Namekata, Y. Takahashi, G. Fujii, D. Fukuda, S. Kurimura, and S. Inoue, *Nat. Photon.* **4**, 655 (2010).
- [22] P. Marek and J. Fiurášek, *Phys. Rev. A* **79**, 062321 (2009).
- [23] D. Stoler, B. E. A. Saleh, and M. C. Teich, *Opt. Acta* **32**, 345 (1985).
- [24] G. S. Agarwal, *Phys. Rev. A* **45**, 1787 (1992).
- [25] P. Adam, J. Janszky, and A. V. Vinogradov, *Phys. Lett. A* **160**, 506 (1991).
- [26] K. L. Pregnell and D. T. Pegg, *Phys. Rev. Lett.* **89**, 173601 (2002).
- [27] L. Memarzadeh and S. Mancini, *Phys. Rev. A* **94**, 022341 (2016).
- [28] H.-C. Fu and R. Sasaki, *J. Phys. Soc. Jpn.* **66**, 1989 (1997).
- [29] I. Urizar-Lanz and G. Tóth, *Phys. Rev. A* **81**, 052108 (2010).
- [30] P. Adam, M. Mechler, V. Szalay, and M. Koniorczyk, *Phys. Rev. A* **89**, 062108 (2014).
- [31] S. Friedland, V. Gheorghiu, and G. Gour, *Phys. Rev. Lett.* **111**, 230401 (2013).
- [32] Y. Yao, X. Xiao, X. Wang, and C. P. Sun, *Phys. Rev. A* **91**, 062113 (2015).
- [33] P. Marek, R. Filip, and A. Furusawa, *Phys. Rev. A* **84**, 053802 (2011).
- [34] K. Miyata, H. Ogawa, P. Marek, R. Filip, H. Yonezawa, J.-i. Yoshikawa, and A. Furusawa, *Phys. Rev. A* **93**, 022301 (2016).
- [35] R. Birrittella, J. Mimih, and C. C. Gerry, *Phys. Rev. A* **86**, 063828 (2012).
- [36] P. A. Knott, T. J. Proctor, A. J. Hayes, J. P. Cooling, and J. A. Dunningham, *Phys. Rev. A* **93**, 033859 (2016).
- [37] S. Olivares, M. Popovic, A. Paris, and G. Matteo, *Quantum Meas. Quantum Metrol.* **3**, 38 (2016).
- [38] T. C. Ralph, A. Gilchrist, G. J. Milburn, W. J. Munro, and S. Glancy, *Phys. Rev. A* **68**, 042319 (2003).
- [39] A. P. Lund, T. C. Ralph, and H. L. Haselgrove, *Phys. Rev. Lett.* **100**, 030503 (2008).
- [40] D. E. Goldberg, *Genetic Algorithms in Search, Optimization and Machine Learning* (Addison-Wesley, Boston, 1989).
- [41] For our calculations, we used the genetic algorithm *ga* from the global optimization toolbox of MATLAB versions 9.2–9.5 (R2017a and b, and R2018a and b) (The Mathworks Inc., Natick, MA).
- [42] P. J. Mosley, J. S. Lundeen, B. J. Smith, P. Wasylczyk, A. B. U'Ren, C. Silberhorn, and I. A. Walmsley, *Phys. Rev. Lett.* **100**, 133601 (2008).
- [43] P. G. Evans, R. S. Bennink, W. P. Grice, T. S. Humble, and J. Schaake, *Phys. Rev. Lett.* **105**, 253601 (2010).
- [44] A. Eckstein, A. Christ, P. J. Mosley, and C. Silberhorn, *Phys. Rev. Lett.* **106**, 013603 (2011).
- [45] P. Adam, M. Mechler, I. Santa, and M. Koniorczyk, *Phys. Rev. A* **90**, 053834 (2014).
- [46] F. Bodog, P. Adam, M. Mechler, I. Santa, and M. Koniorczyk, *Phys. Rev. A* **94**, 033853 (2016).
- [47] H. Yuen and J. Shapiro, *IEEE Trans. Inf. Theor.* **26**, 78 (1980).
- [48] U. Leonhardt and H. Paul, *Phys. Rev. A* **48**, 4598 (1993).
- [49] K. Banaszek and K. Wódziewicz, *Phys. Rev. A* **55**, 3117 (1997).
- [50] J. Appel, D. Hoffman, E. Figueroa, and A. I. Lvovsky, *Phys. Rev. A* **75**, 035802 (2007).